Rigid Spacecraft Formations Actuated by Electric Thrusters with One-Bit Resolution

Edoardo Serpelloni *, Manfredi Maggiore †

and Chris J. Damaren‡

University of Toronto, Toronto, ON, M5S 2J7, Canada.

In this paper we investigate a formation control problem for two space vehicles in general multibody regimes. The objective is to accurately regulate the distance between the vehicles, as well as the orientation of the overall formation to a desired, rigid configuration, under tight tolerances. The propulsion mechanism of each spacecraft is given by a collection of low thrust electric thrusters. We show that the formation control problem is solvable using constant thrust electric actuators requiring only one bit of resolution, overcoming the problem of actuator resolution. The control law we propose is hybrid, and it coordinates the sequence of on-off switches of the thrusters so as to achieve the control objective and, at the same time, avoid sliding modes.

I. Introduction

In the past, several missions for the observation of the universe involving large arrays of spacecraft flying in formation have been proposed. The constraints imposed by the type of observations these missions must perform have led to the identification of trajectories in a neighborhood of the $L2$ lagrangian point of the Sun-Earth/Moon system as an ideal location. NASA proposed, in the context of the Vision Program, the Stellar Imager (SI) mission, a large array of nearly 30 spacecraft flying in formation to form a large telescope.[1] The Terrestrial Planet Finder[2] and the MAXIM[3] mission concepts also involved large formations of spacecraft flying in the vicinity of the $L2$ libration point (small baselines for TPF, very large for MAXIM). These mission concepts share a set of great challenges from the formation control perspective: the type of required scientific observations requires the control of the relative position between spacecraft with submillimetric error tolerances. In particular, the SI vehicles' control systems were supposed to meet three different control specifications,[1] classified as: *rough control*, with accuracy up to a few meters, *intermediate control*, with accuracy in the order of a few centimeters and *fine control*, with submillimeter accuracy.
Each of these control regimes is to be satisfied for an interval of time long enough to allow the scientific observation to be completed (for the SI mission this would depend on the target star rotation period). The problem has been studied deeply in the past, with exploration of a few different strategies. Discrete control methods, such as the Equitime Targeting Method[4,6] and Tangential Targeting Method,[7] implement impulsive maneuvers at various checkpoints along the reference orbit in order to target a relative position Δr between leader and follower. However these methods are not well suited for achieving accuracies at the subcentimeter level.[4] Howell *et al.*,[4,6] proposed the application of Floquet control methods to formations in the vicinity of the reference Halo orbit in order to exploit the structure of the center manifold associated with the orbit itself. These techniques allow one to compute the Δv required to initialize and keep the formation on the center manifold associated with the reference Halo orbit. The elements of the formation will evolve on a torus enveloping the nominal orbit, giving rise to quasi-periodic formations. By properly phasing each vehicle, the formation naturally evolves along the torus so that the relative positions of each spacecraft are unaltered and the relative distances are bounded.
The best performances are, however, guaranteed by the application of continuous control laws. The literature

*PhD Candidate, Electrical and Computer Engineering Department; edoardo.serpelloni@mail.utoronto.ca.
†Professor, Electrical and Computer Engineering Department; maggiore@control.utoronto.ca.
‡Professor, University of Toronto Institute for Aerospace Studies; damaren@utias.utoronto.ca. Associate Fellow AIAA.

about continuous feedback control of formations is massive. However, very little of it is directly applicable to the problem at hand. Marchand and Howell,[5] explored the application of feedback linearization to the control of several different types of formations (aspherical, rigid, etc.). It is shown that the control of the elements of the formation can require thrust levels in the range $nN - mN$. In addition, the robustness of these methods to modeling errors and thrust implementation errors has yet to be explored. Gurfil and Kasdin[8] proposed an optimal controller for a formation of two spacecraft, one of which is free flying along a natural trajectory of the Circular Restricted Three Body Problem (CR3BP). The controller is designed on a time-varying linearization of the CR3BP model about a natural solution. Such controllers require actuators with a dynamic range not achievable with todays's technology. They propose to allocate the required thrust on different propulsive systems on board the spacecraft. Gurfil *et al.*[9] propose an approximate dynamic model inversion combined with linear compensation of the ideal feedback linearized model. Modelling errors and external perturbations are then compensated by a neural network element. Submillimetric tolerances are achieved, assuming thrusters providing continuous thrust in the mN-μN range. However, continuous control laws require the actuators to deliver thrust with prohibitively high resolution for today's technology.[4,8] Actuator resolution is, therefore, the crucial bottleneck in controlling spacecraft formations. A possible way to overcome such a limitation is by using thrusters providing only a constant level of thrust. Stanton and Marchand[10] have proposed a solution based on the numerical optimization of the on-off switching times of each on-board thruster.
In the paper we show that the feedback bang-bang controller presented by the authors in Ref. 11 can be applied to the formation control problem and it is shown that it allows to achieve a formation configuration with virtually any level of accuracy, avoiding sliding modes. This completely eliminates any requirement on the resolution of the on-board thrusters. FEEP (Field Emission Electric Propulsion) thrusters seem to best fit our requirements: they provide very low thrust (in the order of the μN), they are characterized by an almost immediate turning on and turning off and, in addition, they can provide thrust operating in pulse mode.[12,13] Such a control law relies only on the knowledge of the spacecraft attitudes and relative position and velocity. No further parameters or measurements are indeed required. The approach used to derive the control law makes it intrinsically robust to all the perturbations acting on the spacecraft, from solar pressure to the perturbation of additional massive bodies, provided that the propulsive system provides enough thrust. This makes the control law very general and applicable even to formations around a single attractor planet.

II. Formation Control Problem (FCP)

In this Section we present the spacecraft model and all the assumptions related to the vehicles configuration. We then formulate the Formation Control Problem (FCP) and we show that it can be reformulated as an equilibrium stabilization problem.

A. Model and Problem Statement

Consider two spacecraft under the gravitational influence of N massive bodies of the Solar System. In the paper we will use the superscript $(\cdot)^i$ to refer to the i-th spacecraft. We will use interchangeably the notations $(x_1, \ldots, x_n)$ and $[x_1 \ldots x_n]^T$ to indicate vectors in $\mathbb{R}^n$. Let $\mathcal{I}$ denote an inertial reference frame and let $\mathcal{B}^i = \{e_1^i, e_2^i, e_3^i\}$ denote the body frame of the i-th spacecraft, $i = 1, 2$. Let $X^i = (x_1^i, x_2^i, x_3^i)$ and $V^i = (x_4^i, x_5^i, x_6^i)$ denote the position and velocity of spacecraft i with respect to Earth, expressed in frame $\mathcal{I}$, with $i = 1, 2$. The state vector of each spacecraft is taken to be $\chi^i := \mathrm{col}(X^i, V^i) \in \mathbb{R}^6$. Let $r^{j,1}(t)$ be the position vector of planet j with respect to the Earth, expressed in the reference frame $\mathcal{I}$. Let $u^i = (u_1^i, u_2^i, u_3^i)$ be the spacecraft control accelerations expressed in $\mathcal{B}^i$, generated by on-board thrusters. We denote the rotation matrix from frame $\mathcal{B}^i$ to frame $\mathcal{I}$ by R^i. It is assumed here that $R^1 = R^2 = R$, constant. In other words, the two spacecraft have the same, constant, attitude with respect to frame $\mathcal{I}$. The formation control maneuvers proposed in this paper do not change the spacecraft attitude.
The dynamics of the i-th spacecraft is then given by:

$$\begin{aligned} \dot{X}^i &= V^i \\ \dot{V}^i &= G^i(\chi^i, t) + Ru^i, \end{aligned} \tag{1}$$

with

$$G^i(\chi^i, t) = F^i(\chi^i, t) + H^i(\chi^i, t),$$

where $F^i(\chi^i, t)$ models the effects of the gravitational fields of N bodies on the i-th spacecraft,

$$F^i(\chi^i, t) = -\mu_1 \frac{X^i}{||X^i||^3} + \sum_{j=2}^{N} \mu_j \left(\frac{r^{j,1}(t) - X^i}{||r^{j,1}(t) - X^i||^3} - \frac{r^{j,1}(t)}{||r^{j,1}(t)||^3} \right) \tag{2}$$

μ_j is the gravitational parameters of body j, and $H^i(\chi^i, t)$ models all the external disturbances acting on the spacecraft. The model in Eq. (1) represents the standard set of equations of motion for the n-body problem, formulated in frame $\mathcal{I}$ (EPHEM model[4]). We assume that each spacecraft can measure only its relative position and velocity with respect to the other one. We assume also that each spacecraft is equipped with m^i constant-thrust electric thrusters and that the two vehicles are equipped with a total of $m^1 + m^2 = 6$ thrusters. We denote their control acceleration magnitude by $\bar{\omega}$. We can write the i-th input as

$$u^i = \sum_{j=0}^{m^i} \theta_j^i \omega_j^i, \tag{3}$$

where $\theta_j^i \in \mathbb{S}^2$ is the unit vector representing the direction of actuation of the j-th thruster, expressed in the body frame of the i-th spacecraft, while $\omega_j^i \in \{0, \bar{\omega}\}$ represents the on-off state of each thruster. We use the convention that $\theta_0^i \omega_0^i = 0$ (to cover the case $m^i = 0$). Assume here, without loss of generality, that each θ_j^i is aligned with one axis of the $\mathcal{B}^i$ frame, i.e. $\theta_j^i = \pm e_k^i$ for some $k = 1, 2, 3$, with $j \neq 0$. Moreover, we assume that for any $j \leq 6$ there is a unique $0 < \bar{k} \leq 6$ such that $\theta_j \cdot \theta_{\bar{k}} = -1$ (if the associated thrusters are on the same spacecraft) or $\theta_j \cdot \theta_{\bar{k}} = 1$ (if they are on different spacecraft) and $\theta_j \cdot \theta_k = 0$ for all $k \neq \bar{k}, j$.
There are several thrusters distributions that respect this last assumption. Two of these distributions are of particular interest from a practical point of view (Figure 1):

(i) Spacecraft 1 not actuated, while there are six orthonormal thrusters on spacecraft 2, as in Figure 1(a), and

(ii) There are three orthogonally distributed thrusters on both spacecrafts, in the same configuration with respect with their body frames, as in Figure 1(b).

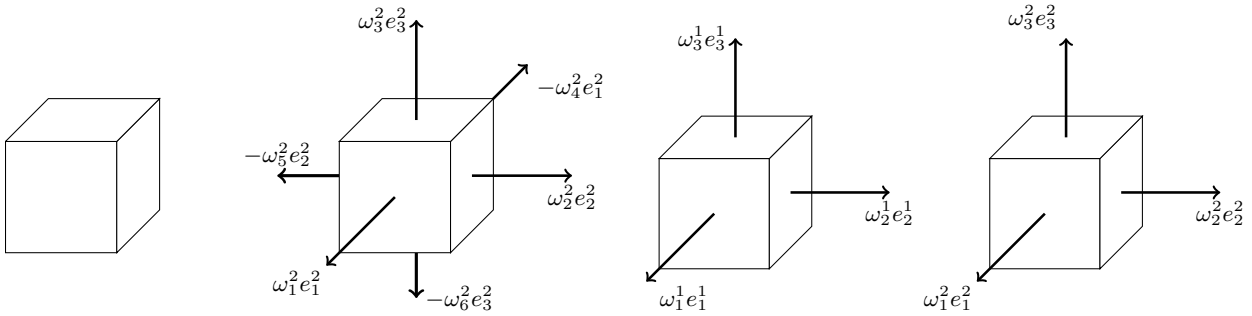

(a) Distribution (i).

(b) Distribution (ii).

Figure 1: Admissible thrusters's deistributions.

Distribution (i) represents the classical leader-follower hierarchical configuration, in which the leader follows a natural orbit, while the follower is controlled in order to meet the formation specifications. Distribution (ii), on the other hand, requires a complete cooperation between the two spacecraft in order to maintain the formation. On the other hand, this configuration requires an additional control layer for the station keeping of the formation. The design of such a control layer will be the subject of future work.
The *distance* d_F between two spacecraft is given by $d_F = \sqrt{(x_1^2 - x_1^1)^2 + (x_2^2 - x_2^1)^2 + (x_3^2 - x_3^1)^2}$. Let α_F be the angle defined as $\alpha_F := \sin^{-1}\left((x_3^2 - x_3^1)/d_F\right)$ and let β_F be the angle $\beta_F := \tan^{-1}\left((x_2^2 - x_2^1)/(x_1^2 - x_1^1)\right)$. We are interested in stabilizing formations of two spacecraft for which d_F, α_F and β_F are constants. Figure

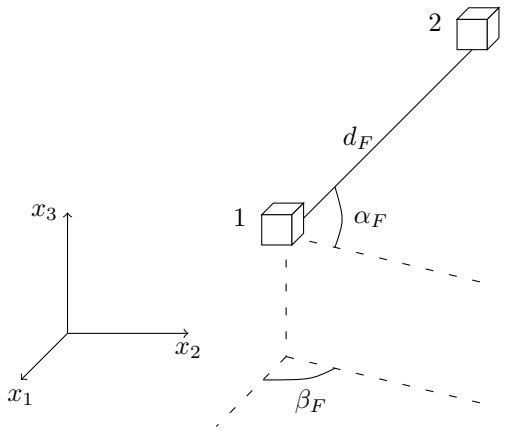

Figure 2: Illustration of the formation configuration parameters (d_F, α_F, β_F).

2 illustrates such a formation configuration. In the following we will specify a desired configuration using the triple (d_F, α_F, β_F).

Formation Control Problem (FCP): Consider two spacecraft modelled as in Eq. (1). Given a desired formation configuration $(\bar{d}_F, \bar{\alpha}_F, \bar{\beta}_F)$ and an associated set of admissible tolerances $(\delta d_F, \delta\alpha_F, \delta\beta_F)$, design the *on-off* switching cycles of each thruster such that the distance between the two spacecraft and the orientation of the formation converge to a neighbourhood $(\bar{d}_F \pm \delta d_F, \bar{\alpha}_F \pm \delta\alpha_F, \bar{\beta}_F \pm \delta\beta_F)$ of the desired rigid formation configuration $(\bar{d}_F, \bar{\alpha}_F, \bar{\beta}_F)$, by switching the on-off state of each thruster with finite frequency.

B. FCP as an equilibrium stabilization problem in relative coordinates

To solve FCP it is convenient to study the relative dynamics of the two spacecraft. To do so we define the relative states $\hat{z}_j$ as

$$\hat{z}_j = x_j^2 - x_j^1, \;\; j = 1, ..., 6$$

We denote the relative state vector by $\hat{\zeta} = \text{col}(\hat{Z}, \hat{V}) \in \mathbb{R}^6$ where states $\hat{Z} = (\hat{z}_1, \hat{z}_2, \hat{z}_3)$ denote the relative position of the second spacecraft with respect to the first one, while states $\hat{V} = (\hat{z}_4, \hat{z}_5, \hat{z}_6)$ denote their relative velocity. The relative dynamics of the two vehicles is then modelled by

$$\begin{aligned} \dot{\hat{Z}} &= \hat{V} \\ \dot{\hat{V}} &= \hat{G}(\hat{\zeta}, \chi^1, t) + R(u^2 - u^1), \end{aligned} \tag{4}$$

where

$$\hat{G}(\hat{\zeta}, \chi^1, t) = G^2(\chi^2, t) - G^1(\chi^1, t).$$

Note that stabilizing the formation $(\bar{d}_F, \bar{\alpha}_F, \bar{\beta}_F)$ in system (1) is equivalent to stabilizing the point $\zeta^\star = (\bar{d}_F \cos(\bar{\alpha}_F)\cos(\bar{\beta}_F), \bar{d}_F \cos(\bar{\alpha}_F)\sin(\bar{\beta}_F), \bar{d}_F \sin(\bar{\alpha}_F), 0, 0, 0)$ for system (4).

Since $\hat{G}(\hat{\zeta}, \chi^1, t)$ is a bounded function (if we exclude a neighbourhood of the planets' centres), we can consider, without any loss in generality, $\hat{G}(\hat{\zeta}, \chi^1, t)$ as an exogenous, bounded, time dependent signal $\hat{G}(t)$. Moreover, by Eq. (3) we can write

$$R(u^2 - u^1) = R\sum_{k=1}^{6} \Theta_k,$$

where

$$\Theta_k = \begin{cases} \theta_k^2 \omega_k^2, & k \leq m^2 \\ -\theta_k^1 \omega_k^1, & k > m^2 \end{cases}$$

This allows us to rewrite Eq. (4) as

$$\begin{aligned}\dot{\hat{Z}} &= \hat{V} \\ \dot{\hat{V}} &= \hat{G}(t) + \bar{\omega} R \begin{pmatrix} \sigma_1 \\ \sigma_2 \\ \sigma_3 \end{pmatrix},\end{aligned} \tag{5}$$

with σ_j be a piecewise constant function with values in $\{-1, 0, 1\}$, $j = 1, 2, 3$. System (5) can be interpreted as a point-mass under the effect of a time-varying acceleration field $\hat{G}(t)$. The vector $\hat{Z} = (\hat{z}_1, \hat{z}_2, \hat{z}_3)$ denotes the position of such a point mass, while $\hat{V} = (\hat{z}_4, \hat{z}_5, \hat{z}_6)$ denotes its velocity. The point-mass in question is fully actuated with on-off thrusters providing a control acceleration $\bar{\omega}$ along three mutually orthogonal directions. Consider now the following coordinate transformation to define a new state $\zeta = (z_1, z_2, z_3, z_4, z_5, z_6) \in \mathbb{R}^6$, $\zeta = T(\hat{\zeta})$, where

$$T : \mathbb{R}^6 \to \mathbb{R}^6, \quad \hat{\zeta} \mapsto \zeta = \begin{bmatrix} R^T & \mathbf{0} \\ \mathbf{0} & R^T \end{bmatrix} (\hat{\zeta} - \zeta^\star) \tag{6}$$

Applying transformation in Eq. (6), the relative dynamics (5) become:

$$\begin{aligned}\dot{z}_1 &= z_4 \\ \dot{z}_2 &= z_5 \\ \dot{z}_3 &= z_6 \\ \dot{z}_4 &= d_1(t) + \bar{\omega}\sigma_1 \\ \dot{z}_5 &= d_2(t) + \bar{\omega}\sigma_2 \\ \dot{z}_6 &= d_3(t) + \bar{\omega}\sigma_3,\end{aligned} \tag{7}$$

where $D(t) = (d_1(t), d_2(t), d_3(t)) = R^T \hat{G}(t)$. Note that $D(t)$ is bounded, and that, under coordinate transformation (6), $T(\zeta^\star) = 0$. The relative dynamics of the spacecraft formation is now written as cascade of double integrators affected by time varying, bounded disturbance signals, modelling the effects of gravity and external disturbances. Since the three double integrators are decoupled, we can achieve the desired formation configuration by designing a practical stabilizer of the origin for the subsystem

$$\begin{aligned}\dot{x}_1 &= x_2 \\ \dot{x}_2 &= d(t) + \bar{\omega}\sigma,\end{aligned} \tag{8}$$

with control input σ having values in $\{-1, 0, +1\}$, and using such controller in each of the subsystems of (7). In the following we denote the solution of system (8) with initial condition x_0 by $\phi_d(t, x_0)$. In light of these observations, FCP can be reformulated as follows.

Revised FCP (RFCP): Consider system (8) with control input σ. Let $d : \mathbb{R} \to \mathbb{R}$ be a measurable function bounded by $\epsilon > 0$. For a given control magnitude $\bar{\omega} > 0$, design a feedback controller with values in $\{-1,\ 0,\ +1\}$ such that:

(i) for all $r > 0$ there exist controller parameters such that for all $x_0 \in \mathbb{R}^2$ and for all $t_0 \in \mathbb{R}$ there exists $T > 0$ such that $\phi(t, t_0, x_0) \in B_r(0)$ for all $t \geq T$,

(ii) given any compact time interval $[t_0, t_1]$, σ switches value with finite frequency.

Note that while specification (i) is related to a stability property that the controller is required to enforce, specification (ii) follows from practical considerations related to the nature of the on-board thrusters. Given the type of electric thrusters on the spacecraft, we must avoid any high frequency switching behaviour. The control system must then be able to reach and stay in a desired neighbourhood of the formation configuration, switching only a finite number of times over a closed interval of time.

III. Main Result

We present here a brief description of the controller implemented to solve the formation control problem (for a more detailed treatment, see Ref. 11).

A. Definitions

Let Γ^+ and Γ^- be the regions depicted in Figure 3. The switching boundary is the set

$$\{(x_1, x_2) \in \mathbb{R}^2 : x_2 = -\text{sign}(x_1)\sqrt{2\bar{\omega}|x_1|}\}$$

It is useful to define the two branches of the switching set as

$$\begin{aligned} s^+ : \mathbb{R}_{>0} \to \mathbb{R}^2 \quad s^+(x) = \left(x, -\sqrt{2\bar{\omega}x}\right) \\ s^- : \mathbb{R}_{<0} \to \mathbb{R}^2 \quad s^-(x) = \left(x, \sqrt{-2\bar{\omega}x}\right) \end{aligned}$$

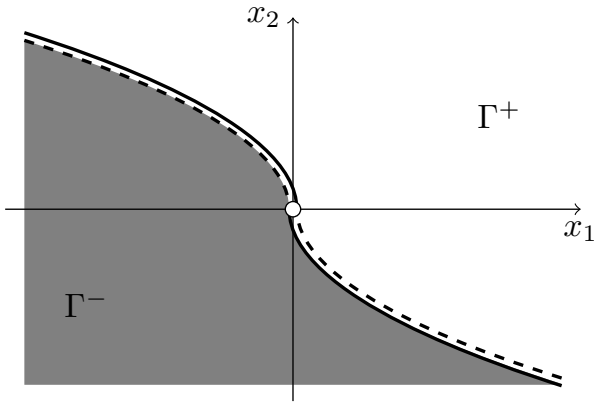

Figure 3: Illustration of the sets Γ^+ and Γ^-. For all $x_1 \in \mathbb{R}_{<0}$, $s^-(x_1) \in \Gamma^+$, while for all $x_1 \in \mathbb{R}_{>0}$, $s^+(x_1) \in \Gamma^-$.

Let sets Σ^- and Σ^+ (shown in Figure 4) be defined as follows

$$\begin{aligned} \Sigma^- &:= \{(x_1, 0) : x_1 \geq 0\} \cup \{s^-(x_1) : x_1 \in \mathbb{R}_{<0}\} \\ \Sigma^+ &:= \{(x_1, 0) : x_1 \leq 0\} \cup \{s^+(x_1) : x_1 \in \mathbb{R}_{>0}\}. \end{aligned} \tag{9}$$

The controller's switching frequency is kept limited by implementing a hysteresis-like mechanism, based on the definition of the two balls $\bar{B}_{\delta_1}(0), B_{\delta_2}(0)$ of radius $0 < \delta_1 < \delta_2$ (shown in Figure 4)

$$\begin{aligned} \bar{B}_{\delta_1}(0) &= \{x \in \mathbb{R}^2 : \|x\| \leq \delta_1\} \\ B_{\delta_2}(0) &= \{x \in \mathbb{R}^2 : \|x\| < \delta_2\} \end{aligned} \tag{10}$$

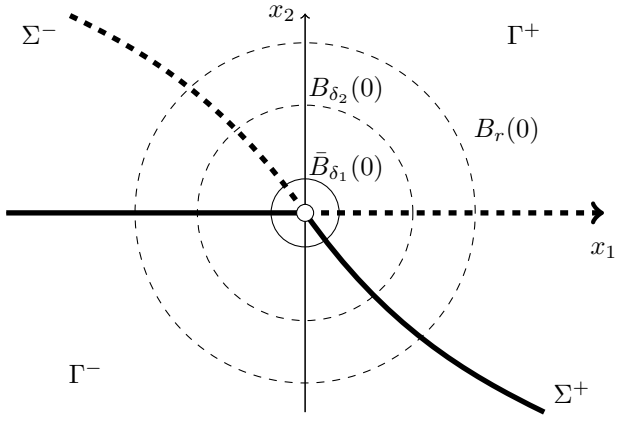

Figure 4: New switching surfaces Σ^+ and Σ^-. Σ^+ is depicted with a solid line, while Σ^- by a dashed line. Open balls $B_r(0)$, $\bar{B}_{\delta_1}(0)$ and $B_{\delta_2}(0)$ are defined in Section III.

In this section we provide a formal structure to the proposed controller together with necessary and sufficient conditions in order to solve RFCP. We moreover present the intuition behind how the controller works.

B. Control Law

We propose a hybrid control law. The introduction of discrete states q_i allows us to efficiently activate and deactivate the switching curves Σ^+, Σ^-. Let $r > \delta_2 > \delta_1 > 0$ be design parameters, where $r > 0$ is the radius of the neighbourhood we want to stabilize, δ_1 is the radius of the open ball in which we choose to turn off the controller, and δ_2 is the radius of the ball outside which the controller is turned on again.

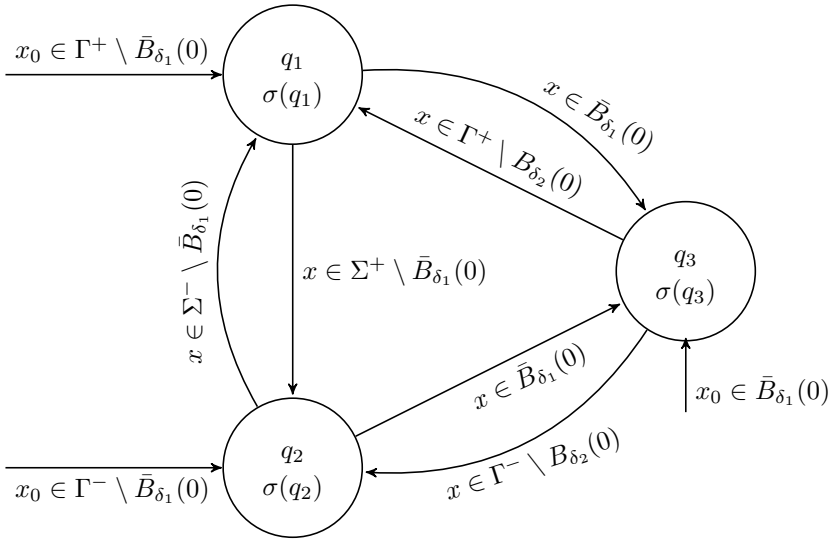

Figure 5: Finite state machine representing the proposed controller. Γ^+ and Γ^- are defined in Figure 3.

The control law is described by the finite state machine in Figure 5, characterized by discrete states $Q = \{q_1, q_2, q_3\}$, continuous states $x \in \mathbb{R}^2$ and hybrid feedback $\sigma(\cdot) : Q \to \mathbb{R}$

$$\begin{aligned} \sigma(q_1) &= -1 \\ \sigma(q_2) &= +1 \\ \sigma(q_3) &= 0 \end{aligned} \tag{11}$$

Referring to Figure 5, if $x_0 \in \Gamma^+$ the discrete state is initialized to q_1 and, as a consequence, the control value is $\sigma(q_1) = -1$. This implies that the switching surface Σ^- is deactivated, meaning that $x \in \Sigma^-$ does not induce a jump in the discrete state. The control value does not change unless one of the guarding conditions is satisfied. If, for example, the state trajectory reaches Σ^+, the discrete state jumps $q_1 \to q_2$, and the control switches accordingly to $\sigma(q_2) = +1$. If, on the other hand, the state trajectory enters $\bar{B}_{\delta_1}(0)$, the discrete state jumps to $q_1 \to q_3$, turning off the controller, $\sigma(q_3) = 0$. The controller stays off unless the state trajectory leaves $B_{\delta_2}(0)$. If that happens, if $x \in \Gamma^+$, $q_3 \to q_1$ and $\sigma(q_1) = -1$, while if $x \in \Gamma^-$, $q_3 \to q_2$ and $\sigma(q_2) = +1$. The process then, continues according to such principles. If δ_1, δ_2 are picked sufficiently small, the state trajectory never leaves $B_r(0)$.
In a mutually exclusive manner, the finite state machine in Figure 5, by means of the discrete states $\{q_1,\ q_2,\ q_3\}$, enables and disables the switching boundaries and regulates the hysteresis of the controller near the origin.

Theorem 1 *There exist $\delta_1 < \delta_2 < r$ such that controller (11) solves RFCP if and only if $\bar{\omega} > \epsilon/2\left(1 + \sqrt{5}\right)$.*

The parameter $\bar{\omega}$ is the thrust magnitude of the spacecraft thrusters. The quantity $\delta_2 < r$ must be chosen sufficiently smaller then r, so that for $\bar{x} \in \partial B_{\delta_2}(0)$, $\phi_d(t, \bar{x})$ stays in $B_r(0)$. The quantity $\delta_1 < \delta_2$ can be chosen arbitrarily. The choice of δ_1 affects the on-off frequency of controller (11) near the origin: a bigger δ_1 will induce a higher switching frequency. A detailed proof of this result can be found in Ref. 11.

IV. Simulations

In this section we present some simulation results in order to prove the effectiveness of controller (11) in keeping a rigid formation of two spacecraft in a neighbourhood of any desired configuration with triple

$(\bar{d}_F, \bar{\alpha}_F, \bar{\beta}_F)$. Let $m_1 = m_2 = 400$ kg be the mass of the two spacecraft. We here assume that the leader (spacecraft 1) is not controlled and follows a Halo orbit around the libration point L_2 of the Sun-Earth/Moon system, Figure 6. We assume here as inertial frame $\mathcal{I}$ an ecliptic frame centered at the Sun. The dynamics

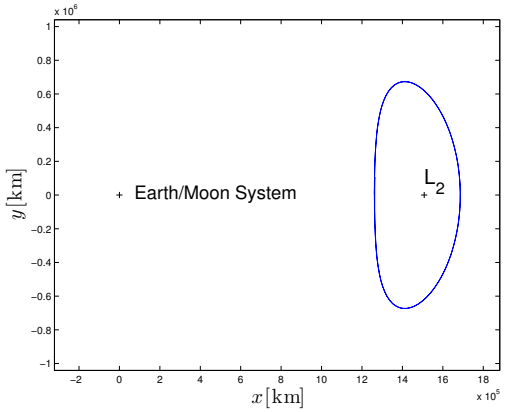

Figure 6: Nominal Halo orbit in the SEM system, as seen in the classical Sun-Earth rotating frame.

of the two vehicles is modelled as in (1). We assume that the follower (spacecraft 2) is fully actuated with a total of 6 electric thrusters providing a constant thrust of $\bar{T} = 40\ \mu N$ each. We let the orientation of the follower with respect to frame $\mathcal{I}$ be represented by the rotation matrix:

$$R = \begin{bmatrix} -0.1808 & -0.4979 & -0.8482 \\ -0.9835 & 0.0915 & 0.1559 \\ 0 & 0.8624 & -0.5063 \end{bmatrix}$$

We assume as target configuration the triple (200 m, $\frac{\pi}{9}$, $\frac{\pi}{6}$), to be kept with tolerance: $\delta d_F = 1$mm, $\delta\alpha_F = 5 \cdot 10^{-6}$ rad, $\delta\beta_F = 5 \cdot 10^{-6}$ rad. Note that we can substitute the open balls $B_{r_i}(0)$ with open boxes U_i defined as $U_i = (-\delta z_i, \delta z_i) \times (-\delta z_{i+3}, \delta z_{i+3})$, where δz_{i+3} is the tolerance in relative velocity. We here then impose: $\delta z_1 = 0.9655 \cdot 10^{-3}$ m, $\delta z_2 = 0.9937 \cdot 10^{-3}$ m, $\delta z_3 = 0.9815 \cdot 10^{-3}$ m, $\delta z_4 = 10^{-5}$ m/s, $\delta z_5 = 10^{-5}$ m/s, $\delta z_6 = 10^{-5}$ m/s.
We assume the relative initial conditions to be given by Table (1):

Table 1: Initial conditions.

Relative state	
$\hat{z}_{1,0}$	244.1393 m
$\hat{z}_{2,0}$	240 m
$\hat{z}_{3,0}$	300 m
$\hat{z}_{4,0}$	$-1.2 \cdot 10^{-3}$ m/s
$\hat{z}_{5,0}$	$-2 \cdot 10^{-3}$ m/s
$\hat{z}_{6,0}$	10^{-4} m/s

The scenario has been simulated for a time interval of $T = 2$ days.
In the following only the results for subsystem $z_1 - z_4$ are presented, in that subsystems $z_2 - z_5$ and $z_3 - z_6$ present similar behavior. Figure 7(a) presents the approaching phase to the desired neighborhood of $(200, \frac{\pi}{9}, \frac{\pi}{6})$ in the relative state ζ. Note that the state trajectories for each individual double integrator subsystem resemble closely the original undirsturbed case, thanks to the low intensity of the gravity differential between the two spacecraft. In all three cases with only one switch per subsystem (3 in total), the formation reaches a neighborhood of the origin.
Figure 7(b) presents the formation keeping phase for subsystem $z_1 - z_4$. It is shown that controller (11) successfully stabilizes the desired neighborhood of the subsystem.

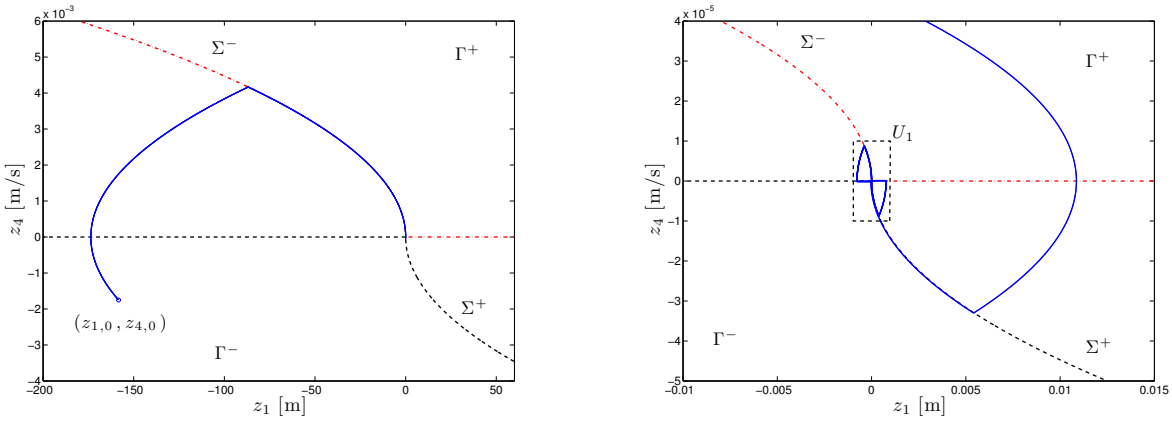

(a) State trajectory of the (z_1, z_4) subsystem.

(b) State trajectory in a neighborhood of U_1.

Figure 7: Approaching phase and formation keeping along for the $z_1 - z_4$ subsystem.

Figure 8(a) presents the time history of the distance $d_F(t)$ between the two spacecraft. The plots for the angles $\alpha_F(t)$ and $\beta_F(t)$ are not shown here, in that they present similar behavior.

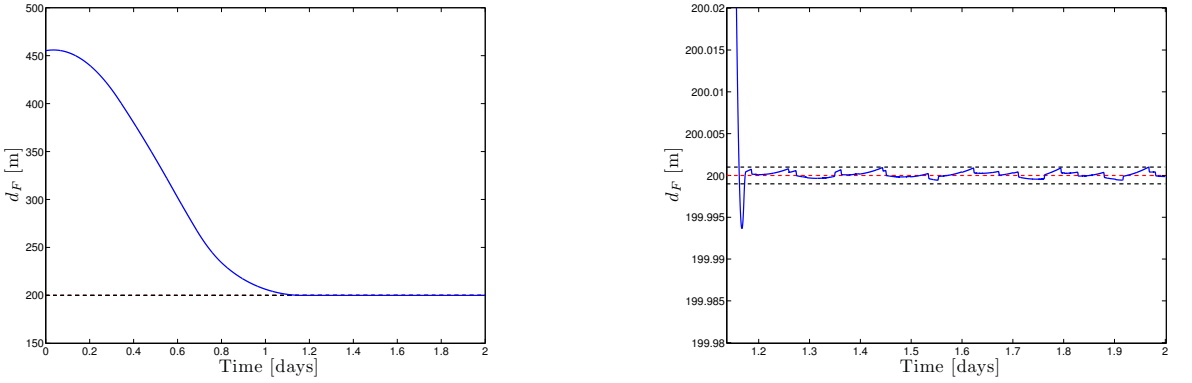

(a) Distance between the two spacecraft $d_F(t)$.

(b) Distance between the two spacecraft $d_F(t)$. After approximately 1.2 days, $d_F(t)$ remains bounded by $\bar{d}_F - \delta d_F$ and $\bar{d}_F + \delta d_F$.

Figure 8: Evolution of the distance between leader and follower.

Figure 8(b) shows that, after approximately 1.2 days, $d_F(t)$ stays in the bound given by the selected tollerances δd_F. This result is met also by $\alpha_F(t)$ and $\beta_F(t)$.
Figure 9 presents the *on-off* switching function of one of the thrusters. The other thrusters present similar behavior, therefore their switching functions are omitted.
Note that the controller is in not forcing any type of high frequency regime in any way. Indeed, as Figure 9 shows, each correction maneuver lasts for a few minutes while the time between two successive accension of the thruster is of the order of one hour.
In concllusion, Figures 7(a) and 7(b) show that controller (11), succesfully achieves and keeps the desired formation configuration meeting the specified tolerance limits, by means of a total of 6 *constant thrust* electric thrusters. In the worst scenario (no intervals with thrusters off), the total cost of the mission would be of approximately $\Delta v = 4.66$ m/s over a timespan of 180 days (the period of the Halo orbit). The cost is then very limited, especially if we consider that such a Δv is to be obtained using electric thrusters. Recent developments in the field of FEEP propulsion systems[13] showed that similar performances can be obtained with just a few grams of propellant. It is interesting to note from Figure 9 that the controller does not

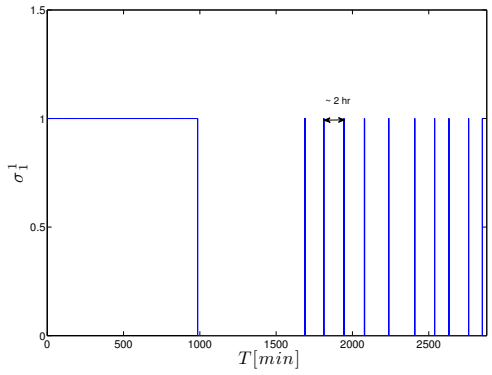

Figure 9: On-off function σ_1^1 for thruster 1.

induce any high frequency behavior and that every maneuver lasts for few seconds/minutes. Moreover, the thrust required is well within the limits of current low thrust technology.

V. Conclusions

The proposed controller overcomes some of the typical issues related to the control of formations along orbits around the libration points. As explained in detail in Section I, the main challenges are not purely theoretical, but they emerge from strong performance constraints imposed by the nature of spacecraft propulsion systems. Controller (11) allows us to keep the formation, meeting very tight tolerances in terms of the accuracy in the control of the distance between the two spacecraft and their orientation, while using thrusters providing just a constant amount of thrust. This allows us to completely disregard any requirements in terms of the resolution of the onboard thrusters. This feature is important when compared to the requirements imposed by classic, continuous control laws. The structure of the controller, in addition, allows, through a proper selection of the parameters r, δ_1 and δ_2, to meet all the different control specifications explained in Section I. In addition, controller (11) requires only the information of the two spacecraft attitude and relative position and velocity. No further measurements are required. As shown in simulations, the thrust magnitude required by controller (11) in order to keep the formation is well within the performances of today's electric thrusters (FEEP thrusters in particular seem to fit particularly well in this scenario.[12,13] As shown in Figure 9, the controller does not induce any high frequency switching. Each small correction is implemented in the time range of few seconds or minutes. Obviously, the number of maneuvers increases as the tolerance on distance and orientation decrease.

References

[1]Carpenter, K. G., Schrijver, C. J. and Karovska, M., "The stellar imager (SI) vision mission," *Proceedings of the SPIE 6268, Advances in Stellar Interferometry*, SPIE, pp. 626821-626821-12, 2006.

[2]Coulter, Daniel R., "NASA's Terrestrial Planet Finder mission: the search for habitable planets," *Proceedings of the SPIE 5487, Optical, Infrared, and Millimeter Space Telescopes*, SPIE, Vol. 539, 2003.

[3]Gendreau, K. C., Cash, W. C., Shipley, A. F., and White, N., "MAXIM Pathfinder x-ray interferometry mission," *Proceedings of the SPIE 4851, X-Ray and Gamma-Ray Telescopes and Instruments for Astronomy*, SPIE, pp. 353-364, 2003.

[4]Howell, K. C. and Marchand, B. G., "Natural and non-natural spacecraft formations near the L1 and L2 libration points in the Sun–Earth/Moon ephemeris system," *Dynamical Systems: An International Journal*, Vol. 20, no. 1, pp. 149-173, 2005.

[5]Marchand, B.G., and Howell, K., "Control Strategies for Formation Flight in the Vicinity of the Libration Points," *Journal of Guidance, Control, and Dynamics*, Vol. 28, no. 6, pp. 1210-1219, 2005.

[6]Millard, L. D. and Howell, K. C., "Control of interferometric spacecraft arrays for (u, v) plane coverage in multi-body regimes," *The Journal of the Astronautical Sciences*, Vol. 56, no. 1, pp. 71-97, 2008.

[7]Qi, R., Xu, S. and Xu, M., "Impulsive Control for Formation Flight About Libration Points," *Journal of Guidance, Control, and Dynamics*, Vol. 35, no. 2, pp. 484-496, 2012.

[8]Gurfil, P. and Kasdin, N. J., "Stability and control of spacecraft formation flying in trajectories of the restricted three-body problem," *Acta Astronautica*, Vol. 54, no. 6, pp. 433-453, 2004.

[9]Gurfil, P., Idan, M. and Kasdin, N. J., "Adaptive neural control of deep-space formation flying," *Journal of Guidance,*

Control, and Dynamics, Vol. 26, no. 3, pp. 491-501, 2003.

[10]Stanton, S. A. and Marchand, B., "Actuator Constrained Optimal Control of Formations Near the Libration Points," *AIAA/AAS Astrodynamics Specialist Conference and Exhibit*, 2008.

[11]Serpelloni, E., Maggiore, M. and Damaren, C.J., "Bang bang hybrid stabilization of perturbed double integrators," to appear in *Proceedings of the* 53^{rd} *IEEE Conference on Decision and Control*, 2014.

[12]Marcuccio, S., Genovese, A. and Andrenucci, M., "Experimental performance of field emission microthrusters," *Journal of Propulsion and Power*, Vol. 14, no. 5, pp. 774-781, 1998.

[13]Paita, L., Ceccanti, F., Spurio, M., Cesari, U., Priami, L., Nania, F. and Andrenucci, M., "Alta's FT-150 FEEP microthruster: development and qualification status," In *Proceeding of the International Electric Propulsion Conference*, IEPC-09-186, 2009.

[14]Bryson, A. E. and Ho, Y. C., "Applied optimal control: optimization, estimation, and control," Taylor & Francis. Chicago, 1975.

[15]Rao, V. G. and Bernstein, D. S., "Naive control of the double integrator," *IEEE Control Systems*, Vol. 21, no. 5, pp. 86-97, 2001.

[16]Goebel, R., Sanfelice, R. G. and Teel, A., "Hybrid dynamical systems," *IEEE Control Systems,* Vol. 29, no. 2, pp. 28-93, 2009.

[17]Maggiore, M., Rawn, B.G. and Lehn, P.G., "Invariance Kernels of Single-Input Planar Nonlinear Systems," *SIAM Journal on Control and Optimization*, Vol. 50, no. 2, pp. 1012-1037, 2009.